

A Multi-Day Wearable Surface EMG E-Tattoo for Fatigue Monitoring*

Heeyong Huh¹, Xiangxing Yang², Hyonyoung Shin², and Nanshu Lu^{1,2,3,4,5}

Abstract—Surface electromyography (sEMG) is a commonly used technique for the non-invasive measurement of muscle activity. However, the traditional electrodes used for sEMG often have limitations regarding their long-term wearability. This study explored the feasibility of a wearable platform using a tattoo-like epidermal electrode (e-tattoo) for multi-day sEMG monitoring. Our sEMG e-tattoo provided stable and reliable sEMG signals over three days of application comparable to conventional gel electrodes. In addition, the e-tattoo has great resistance to motion artifacts and, therefore, maintains a high signal-to-noise ratio (SNR) and signal-to-motion ratio (SMR) during dynamic activities such as cycling. This robust wearable platform opens up new avenues for developing future wearable sEMG devices and advancing dynamic muscle fatigue research.

Clinical relevance—The proposed wearable sEMG system can provide continuous and non-invasive monitoring of muscle activity, providing insights for improving rehabilitation and EMG-based prosthesis development for patients.

I. INTRODUCTION

Extreme fatigue at work sites increases the risk of injury and decreases productivity. To address this challenge, wearable electronics have emerged as a promising solution to monitor the muscle condition of workers engaged in physically demanding tasks, such as at distribution centers and construction sites, through surface electromyography (sEMG). Although there were many proposed studies on the correlation between characteristics of sEMG and muscle fatigue, most studies were limited to short-term fatigue under muscle contraction with a limited range of motion [1], [2], [3], [4]. One of the major limitations of these studies is the absence of a robust sEMG system for long-term monitoring. Conventional gel-based wet electrodes are uncomfortable, bulky, and prone to dehydration, which limits their use for extended periods [5].

Recently, advancements in materials and fabrication methods have made dry electrodes, known as e-tattoos (electronic tattoos), a more viable solution for comfortable and long-term monitoring while ensuring high-quality signals [6], [7], [8], [9], [10]. However, the system-level integration of such e-tattoos into practical devices still remains challenging.

Reliable data acquisition (DAQ) during dynamic activities requires stable connections between the ultrathin, soft e-tattoos and the millimeter-thick, rigid printed circuit boards

(PCB) in order to be free from motion and other ambient artifacts. Previously, flexible interconnections between the e-tattoos with a gradual increase in thickness were proposed to minimize Young’s modulus mismatch between layers [11], [12], [13]. Still, these connectors are time-consuming to manufacture and difficult to deploy in long-term applications.

To address these challenges, this work presents an sEMG e-tattoo with a high signal-to-noise ratio (SNR) comparable to the gold-standard gel electrodes and a high signal-to-motion ratio (SMR) that minimizes dynamic motion-induced artifacts. The cost-effective and simple connection between the electrodes and the flexible printed circuit (FPC) interconnector minimizes motion artifacts without compromising softness. The plug-and-play analog front end (AFE) is designed to be user-centered, improving accessibility for multi-day use. Furthermore, this study showcased the capability of the sEMG e-tattoo system to drive innovation in future multi-day muscle fatigue research.

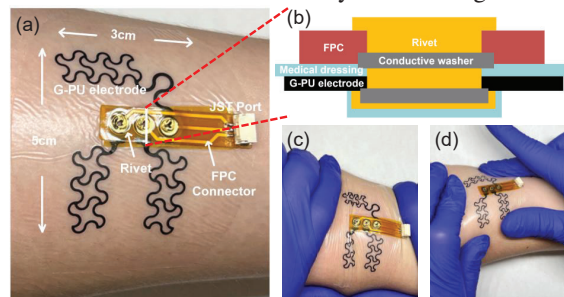


Fig. 1. (a) Soft, stretchable sEMG e-tattoo with a flexible FPC interconnector. (b) Side view of the connection between electrodes and the FPC interconnector. E-tattoo under (c) stretching and (d) twisting on skin.

II. MATERIALS AND METHODS

A. sEMG E-tattoo Design

The sEMG e-tattoo is depicted in Fig. 1a. The electrodes are made of a 50- μm -thick serpentine patterned conductive graphite deposited polyurethane (G-PU) film and supported by a medical dressing (Tegaderm, 3M), resulting in a soft, skin-friendly patch that can be worn for extended periods.

Previous electrical connections for thin-film sensors, such as epoxy-based solder and anisotropic conductive film [12], [13], are not robust enough for long-term wear and endure cyclic load applied under frequent movements. Instead, the rivet connection in Fig. 1b provides a secure link between the soft e-tattoo and the FPC interconnector. The JST-GH port offers a user-friendly plug-and-play interface to the AFE and DAQ system for practical use. Despite the rigid rivet connection, the e-tattoo remains flexible, able to accommodate skin movements like stretching (Fig. 1c) and twisting (Fig. 1d).

B. Analog Front-End Design

The AFE shown in Fig. 2 includes four stages for analog domain signal processing: an instrumentation amplifier, 60

*This work was supported by Office of Naval Research (ONR), USA

¹Department of Aerospace Engineering and Engineering Mechanics, The University of Texas at Austin, Austin, TX 78712, USA.

²Department of Electrical and Computer Engineering, The University of Texas at Austin, Austin, TX 78712, USA.

³Department of Mechanical Engineering, The University of Texas at Austin, Austin, TX 78712, USA.

⁴Department of Biomedical Engineering, The University of Texas at Austin, Austin, TX 78712, USA.

⁵Texas Materials Institute, The University of Texas at Austin, Austin, TX 78712, USA.

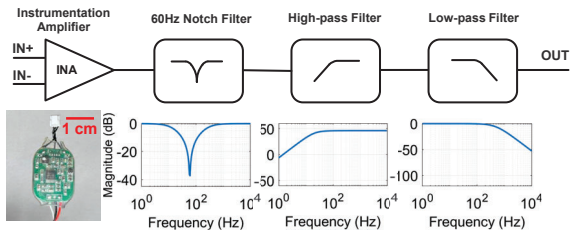


Fig. 2. The AFE, with a compact design, amplifies the sEMG band of 20-480 Hz.

Hz notch filter, high-pass filter, and low-pass filter. The instrumentation amplifier provides high input impedance and common mode rejection. A relatively low input stage gain of 19 was used to avoid saturating the amplifier. The second stage was a notch filter implemented by a twin-T network and a source follower. The center rejection frequency was set to 60 Hz to eliminate power line interference. The high-pass stage was designed with a Sallen-Key topology, with a gain of 200 and a cutoff frequency of 20 Hz. The low-pass stage was also designed with Sallen-Key topology, with unity gain and a cut-off frequency of 480 Hz.

C. Subject and Study Procedure

Five healthy subjects (males, age 22 ± 4 years) participated in a three-day exercise study. E-tattoos and conventional gel electrodes were applied to the vastus lateralis muscle for comparison. During the study, subjects wore the sensors continuously and were allowed to engage in usual daily activities, including showering. However, they were asked to avoid intense exercises that could fatigue the leg muscles. The subjects performed 30 squats and all-out one-minute power cycling daily for three days, and the sEMG signal and the contact impedance were collected. The experimental procedures involving human subjects described in this paper were approved by the University of Texas at Austin Institutional Review Board.

The long-term stability of the sEMG e-tattoos was evaluated using two criteria: secure contact of electrodes on the skin and signal quality. Electrode-skin contact was assessed by measuring the contact impedance over time,

while signal quality was evaluated by computing the signal-to-noise ratio (SNR) and the stability of the myoelectric signal relative to motion (SMR). Contact impedance was measured by applying a 1 kHz sinusoidal current between the sEMG input electrodes.

The SNR and SMR were computed for each contraction of the muscle. The SNR was calculated by dividing the total power of the sEMG signal across all frequencies by the power of the noise frequency range, which is assumed to be ambient noise in the upper 20% of the frequency range (above 400 Hz) [14]. To evaluate signal stability from the motion artifacts, the SMR was computed as the ratio of total sEMG power to the motion-induced noise power, which was calculated as the sum of the power spectral density (PSD) area below 20 Hz and above a straight line connecting the origin and the peak power between 50 Hz and 150 Hz [15].

D. Signal Processing

The AFE-preamplified sEMG signals were sampled at 1 kHz using a data acquisition (DAQ) system (NI-DAQ, National Instruments). The raw sEMG signals were detrended and then squared to segment the muscle contractions. For each contraction, the mean frequency (MNF) and median frequency (MDF) were computed by fast Fourier transform. The average root-mean-squared (RMS) of each contraction was computed as well. The raw signals were also decomposed by empirical mode decomposition (EMD), which can separate a time series into a set of oscillatory components in different frequencies, called intrinsic mode functions (IMFs) [16].

III. RESULTS AND DISCUSSION

A. Multi-day Signal Reliability

The electrode-skin contact impedance is a standard metric for evaluating electrodes' skin conformability and conductivity. Lowering the contact impedance improves signal quality. We compared the impedance of the e-tattoos and the conventional gel electrodes for both short-term and long-term periods.

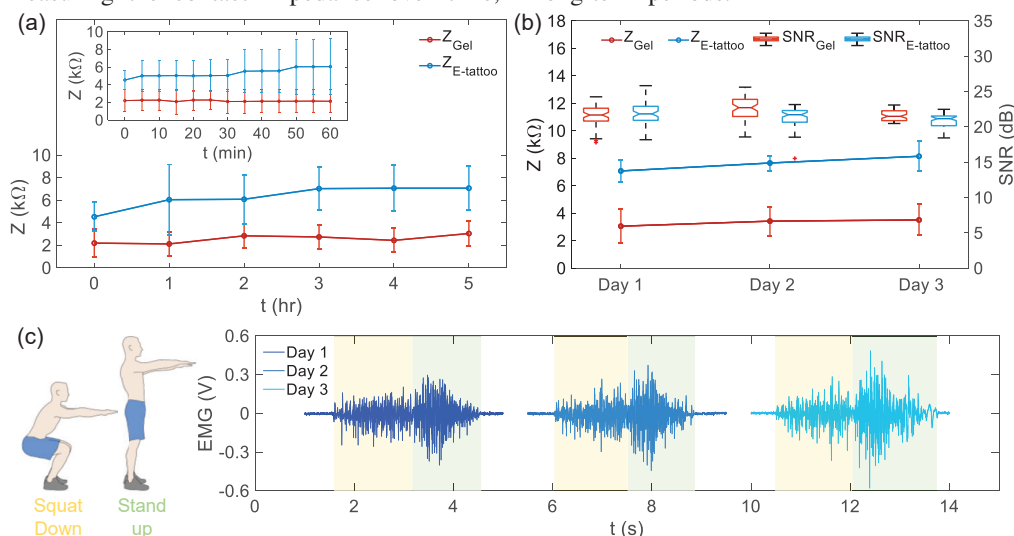


Fig. 3. (a) The contact impedance over the first one hour (inset) and five hours. (b) The contact impedance and SNR of the sEMG signal during three days of the squat exercise. (c) The raw sEMG signals during three days of the squat exercise.

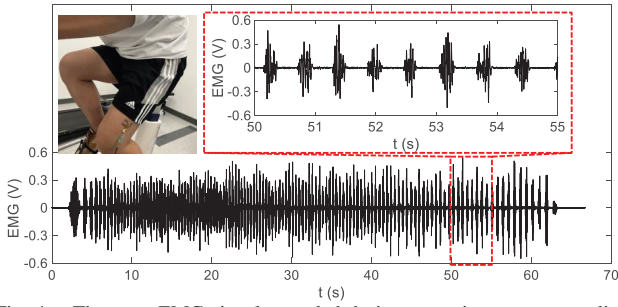


Fig. 4. The raw sEMG signal recorded during one-minute power cycling shows clear muscle activation without motion artifacts.

As shown in Fig. 3a, both e-tattoos and gel electrodes had low initial impedance, with an average of 4.54 k Ω and 2.21 k Ω respectively. Over time, the impedance increased gradually for both electrodes, with the e-tattoo stabilizing at 7.08 k Ω and the gel electrode at 3.06 k Ω after 5 hours.

The contact impedance increased less than 5 k Ω over three days, demonstrating the multi-day reliability of the e-tattoo. Although the contact impedance of the dry e-tattoo electrode was higher than that of the wet gel electrode, the SNRs of both electrodes were comparable over the three days, as shown in the notched box plots in Fig. 3b. On the first day, the average SNR was 21.84 dB for the e-tattoo and 21.59 dB for the gel electrode. By the third day, the average SNRs had decreased slightly to 20.78 dB and 21.58 dB, respectively. The SNR of each muscle contraction was above 15 dB, indicating that the sEMG signals were not severely contaminated by noise during dynamic muscle contractions [14]. Fig. 3c also shows that the amplitude of the baseline and EMG contractions remained consistent over three days of measurement using the e-tattoo.

B. Multi-day Muscle Fatigue Monitoring

Because our robustly designed e-tattoo endures on-skin deformation, it acquires reliable sEMG even during highly dynamic activities. In our study, the subjects performed a one-minute power cycling test to induce leg muscle fatigue while sEMG signals were recorded using the e-tattoo system.

Fig. 4 shows raw sEMG signal from a subject during the cycling test. Despite the subjects maintaining a high speed of 2-4 cycles per second, muscle contractions are clearly distinguishable without any noticeable motion artifacts, as shown in the zoomed-in inset of Fig. 4. The MNF and MDF of the raw signal and the first three IMFs of muscle contractions are shown in Fig. 5. The MNF of the sEMG decreases as fatigue accumulates over time in all IMFs [17], with IMF1 decaying faster than IMF2 and IMF3, suggesting that higher frequency components of EMG are more sensitive to muscle fatigue. MDF also decreased in all IMFs but decreased more gradually than MNF. In fact, the decay slopes were similar in all IMFs and the raw signal. The features' variance was greater in the IMF1 than in the IMF2 and IMF3.

Fig. 6 shows that the SNR and SMR of muscle contractions during cycling decreased over three days. Such a decrease can be explained by an increase in contact impedance which made the e-tattoo more susceptible to ambient noise. The SNR and SMR values remained

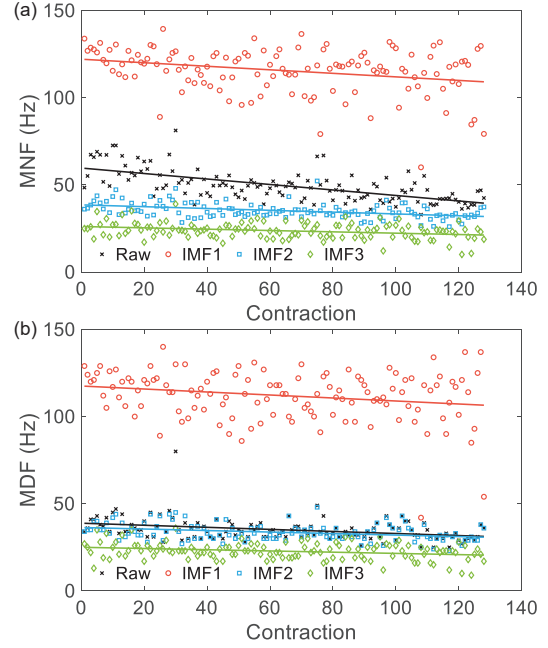


Fig. 5. The decreases in the (a) MNF and (b) MDF of the raw signal and the first three IMFs indicate muscle fatigue during one-minute power cycling.

above 15 dB and 12 dB, respectively, which indicate an acceptable sEMG signal with little influence of artifacts [14]. This demonstrates the stability of the sEMG e-tattoo for multi-day dynamic muscle activity monitoring.

Lastly, we investigated the change in the MNF, MDF, and RMS values of muscle contractions over three days of exercise. Fig. 7 shows that the MNF and MDF decreased while the RMS increased as fatigue progressed [18]. The slopes of the linear fit lines become flatter over days. The MNF and MDF of the early muscle contractions during the cycling task were higher on the first day than on the following days. On the other hand, they converge to similar values towards the end of the task. This may indicate that the muscle was not fully recovered from the fatigue between days, and there is a lower bound of the sEMG frequency spectrum at the fatigue state. The initial RMS values were also higher on later days, indicating muscle fatigue accumulation during multi-day exercises. Although a decrease in the MNF and MDF and an increase in the RMS of an EMG signal are well-known characteristics of muscle fatigue, a correlation between sEMG features and multi-day fatigue and recovery has yet to be fully explored due to the current limitation of the conventional

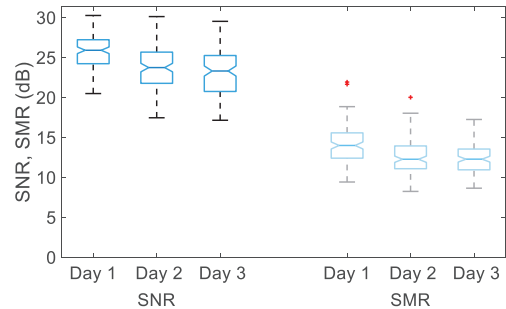


Fig. 6. The e-tattoo maintains acceptable SNR and SMR during three-day cycling exercises.

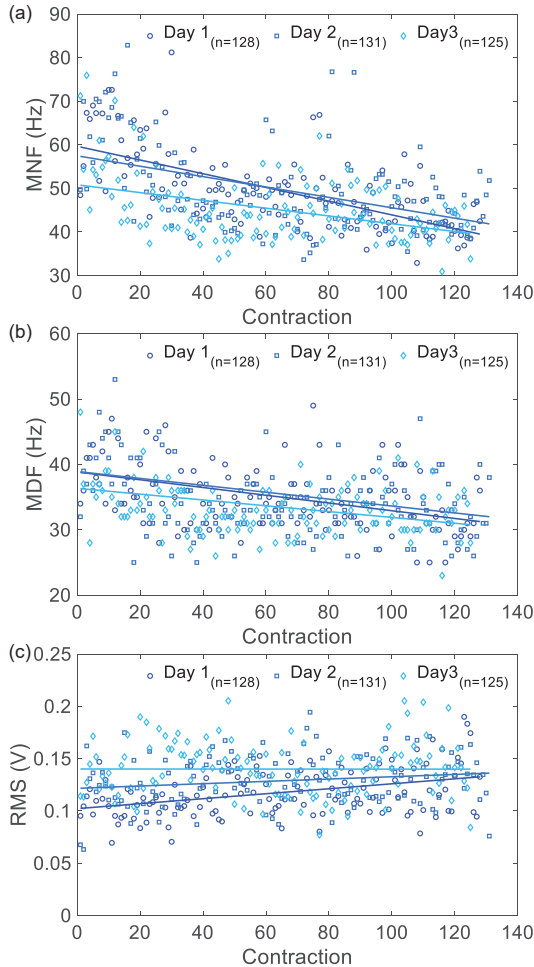


Fig. 7. The different initial values of various sEMG features indicate accumulation of muscle fatigue during three-day cycling exercises. The initial values of the (a) MNF and (b) MDF decreases over three days. (c) The initial value of RMS increases over three days.

sEMG hardware. Thus, the proposed sEMG e-tattoo system provides a promising approach for stable and non-invasive monitoring of muscle activities for clinical applications.

IV. CONCLUSIONS

In this paper, we developed an sEMG e-tattoo electrode with a robust interconnector for multi-day muscle activity monitoring. The results of high SNR and SMR during dynamic exercise demonstrate the device's ability to resist ambulatory noises. We also evaluated the system's performance in monitoring muscle fatigue during multi-day dynamic exercise. While changes in the MNF, MDF, and RMS of the EMG signals under muscle fatigue and during dynamic activities have been investigated, their explicit correlation with multi-day fatigue accumulation is yet to be established due to limitations in stable EMG monitoring under various conditions. To fully understand the correlation between these EMG features and muscle fatigue influenced by a variety of factors, further development of wearable continuous monitoring platforms that can collect ample data over an extended period is necessary.

ACKNOWLEDGMENT

This work was supported by grants from the Office of Naval Research (ONR), USA (grant number N00014-20-1-

2112). We would like to thank the study subjects for their voluntary participation.

REFERENCES

- [1] H. Jebelli and S. Lee, "Feasibility of wearable electromyography (emg) to assess construction workers' muscle fatigue," in *Advances in Informatics and Computing in Civil and Construction Engineering: Proceedings of the 35th CIB W78 2018 Conference: IT in Design, Construction, and Management*. Springer, 2019, pp. 181–187.
- [2] M. A. Nussbaum, "Static and dynamic myoelectric measures of shoulder muscle fatigue during intermittent dynamic exertions of low to moderate intensity," *European journal of applied physiology*, vol. 85, pp. 299–309, 2001.
- [3] L. Wang, Y. Wang, A. Ma, G. Ma, Y. Ye, R. Li, and T. Lu, "A comparative study of emg indices in muscle fatigue evaluation based on grey relational analysis during all-out cycling exercise," *BioMed research international*, vol. 2018, 2018.
- [4] S.-H. Liu, C.-B. Lin, Y. Chen, W. Chen, T.-S. Huang, and C.-Y. Hsu, "An emg patch for the real-time monitoring of muscle-fatigue conditions during exercise," *Sensors*, vol. 19, no. 14, p. 3108, 2019.
- [5] Y. Fu, J. Zhao, Y. Dong, and X. Wang, "Dry electrodes for human bioelectrical signal monitoring," *Sensors*, vol. 20, no. 13, p. 3651, 2020.
- [6] Y. Wang, L. Yin, Y. Bai, S. Liu, L. Wang, Y. Zhou, C. Hou, Z. Yang, H. Wu, J. Ma *et al.*, "Electrically compensated, tattoo-like electrodes for epidermal electrophysiology at scale," *Science Advances*, vol. 6, no. 43, p. eabd0996, 2020.
- [7] H. Liu, W. Dong, Y. Li, F. Li, J. Geng, M. Zhu, T. Chen, H. Zhang, L. Sun, and C. Lee, "An epidermal semg tattoo-like patch as a new human-machine interface for patients with loss of voice," *Microsystems & nanoengineering*, vol. 6, no. 1, p. 16, 2020.
- [8] Y. Zhang and T. H. Tao, "Skin-friendly electronics for acquiring human physiological signatures," *Advanced Materials*, vol. 31, no. 49, p. 1905767, 2019.
- [9] E. Bihar, T. Roberts, Y. Zhang, E. Ismailova, T. Herve, G. G. Malliaras, J. B. De Graaf, S. Inal, and M. Saadaoui, "Fully printed all-polymer tattoo/textile electronics for electromyography," *Flexible and Printed Electronics*, vol. 3, no. 3, p. 034004, 2018.
- [10] G.-H. Lee, Y. R. Lee, H. Kim, D. A. Kwon, H. Kim, C. Yang, S. Q. Choi, S. Park, J.-W. Jeong, and S. Park, "Rapid meniscus-guided printing of stable semi-solid-state liquid metal microgranular-particle for soft electronics," *Nature Communications*, vol. 13, no. 1, p. 2643, 2022.
- [11] H. Jang, K. Sel, E. Kim, S. Kim, X. Yang, S. Kang, K.-H. Ha, R. Wang, Y. Rao, R. Jafari *et al.*, "Graphene e-tattoos for unobstructive ambulatory electrodermal activity sensing on the palm enabled by heterogeneous serpentine ribbons," *Nature Communications*, vol. 13, no. 1, p. 6604, 2022.
- [12] O.-H. Huttunen, M. H. Behfar, J. Hiitola-Keinänen, and J. Hiltunen, "Electronic tattoo with transferable printed electrodes and interconnects for wireless electrophysiology monitoring," *Advanced Materials Technologies*, vol. 7, no. 8, p. 2101496, 2022.
- [13] J. H. Shin, J. Kwon, J. U. Kim, H. Ryu, J. Ok, S. Joon Kwon, H. Park, and T.-i. Kim, "Wearable eeg electronics for a brain-ai closed-loop system to enhance autonomous machine decision-making," *npj Flexible Electronics*, vol. 6, no. 1, p. 32, 2022.
- [14] C. Sinderby, L. Lindstrom, and A. Grassino, "Automatic assessment of electromyogram quality," *Journal of Applied Physiology*, vol. 79, no. 5, pp. 1803–1815, 1995.
- [15] H. F. Posada-Quintero, R. T. Rood, K. Burnham, J. Pennace, and K. H. Chon, "Assessment of carbon/salt/adhesive electrodes for surface electromyography measurements," *IEEE journal of translational engineering in health and medicine*, vol. 4, pp. 1–9, 2016.
- [16] N. E. Huang, Z. Shen, S. R. Long, M. C. Wu, H. H. Shih, Q. Zheng, N.-C. Yen, C. C. Tung, and H. H. Liu, "The empirical mode decomposition and the hilbert spectrum for nonlinear and non-stationary time series analysis," *Proceedings of the Royal Society of London. Series A: mathematical, physical and engineering sciences*, vol. 454, no. 1971, pp. 903–995, 1998.
- [17] R. M. Enoka and J. Duchateau, "Muscle fatigue: what, why and how it influences muscle function," *The Journal of physiology*, vol. 586, no. 1, pp. 11–23, 2008.
- [18] M. Cifrek, V. Medved, S. Tonković, and S. Ostojčić, "Surface emg based muscle fatigue evaluation in biomechanics," *Clinical biomechanics*, vol. 24, no. 4, pp. 327–340, 2009.